AIP Advances

Effect of growth temperature on defects in epitaxial GaN film grown by plasma assisted molecular beam epitaxy

S. S. Kushvaha, P. Pal, A. K. Shukla, Amish G. Joshi, Govind Gupta, M. Kumar, S. Singh, Bipin K. Gupta, and D. Haranath

Citation: AIP Advances **4**, 027114 (2014); doi: 10.1063/1.4866445
View online: http://dx.doi.org/10.1063/1.4866445
View Table of Contents: http://scitation.aip.org/content/aip/journal/adva/4/2?ver=pdfcov
Published by the AIP Publishing

AIP ADVANCES **4**, 027114 (2014)

Effect of growth temperature on defects in epitaxial GaN film grown by plasma assisted molecular beam epitaxy

S. S. Kushvaha,[a] P. Pal, A. K. Shukla, Amish G. Joshi, Govind Gupta, M. Kumar, S. Singh, Bipin K. Gupta, and D. Haranath
CSIR- National Physical Laboratory, Dr. K. S. Krishnan Road, New Delhi, India 110012

(Received 20 December 2013; accepted 7 February 2014; published online 18 February 2014)

We report the effect of growth temperature on defect states of GaN epitaxial layers grown on 3.5 μm thick GaN epi-layer on sapphire (0001) substrates using plasma assisted molecular beam epitaxy. The GaN samples grown at three different substrate temperatures at 730, 740 and 750 °C were characterized using atomic force microscopy and photoluminescence spectroscopy. The atomic force microscopy images of these samples show the presence of small surface and large hexagonal pits on the GaN film surfaces. The surface defect density of high temperature grown sample is smaller (4.0×10^8 cm^{-2} at 750 °C) than that of the low temperature grown sample (1.1×10^9 cm^{-2} at 730 °C). A correlation between growth temperature and concentration of deep centre defect states from photoluminescence spectra is also presented. The GaN film grown at 750 °C exhibits the lowest defect concentration which confirms that the growth temperature strongly influences the surface morphology and affects the optical properties of the GaN epitaxial films. [http://dx.doi.org/10.1063/1.4866445]

I. INTRODUCTION

The GaN-based semiconductor materials have been attracting immense interest particularly due to their importance in many applied fields such as ultraviolet light emitting diodes, high electron mobility transistors, optical data storage and related devices.[1–6] The minimization of the defects and obtaining the smooth film with high structural quality of GaN surface are the key factors for realization of high performance GaN based devices. The defects are main concern for several reasons. The defects cause large leakage current and thereby degrading the performance of the devices. In GaN epilayers, these defects are expected to affect the electronic structure and optical properties. Therefore, the defects in the grown film become a critical issue for the devices. There are a number of reports related to the studies of quantitative analysis of defects concentration.[7,8] However, the influence of growth temperature on defect concentration and the nature of the mid-gap defect states are less explored.[9,10]

Atomic force microscopy (AFM) characterization is one of the surface characterization techniques to study the surface morphology, roughness and the surface defects/dislocation density on GaN epitaxial film.[2,11,12] The surface pits and hexagonal pits has been characterized by AFM on GaN film grown by metal organic chemical vapor deposition (MOCVD) and molecular beam epitaxy (MBE).[2,11–15] In these studies, the formations of hexagonal shaped pits are attributed to the presence of screw/mixed threading dislocations in GaN films.[2,14] In addition, *ex-situ* AFM characterization has been typically used to optimize the growth conditions such as Ga/N flux ratio and growth temperatures to obtain high quality epitaxial films.[14] Apart from the surface defects, the optical properties are strongly influenced by the growth temperature and these can be easily probed using photoluminescence (PL) spectroscopy. There are many experimental investigations on the optical

[a]Electronic mail: kushvahas@nplindia.org

properties using PL which show that the PL spectra are sensitive to the changes in the mid-gap defect states. Grieshaber *et al.*[16] have shown that there are two different luminescence centres present in GaN epilayers, one centered at 3.4 eV and other centered at 2.2 eV. The peak at 3.4 eV is mainly due to the band to band transition and the 2.2 eV peak has contributions from the intrinsic defect states.

In this paper, we report the effect of growth temperature on the defects in the epitaxial GaN films grown using plasma assisted molecular beam epitaxy (PAMBE). The structural and optical properties of the GaN films were characterized using AFM and PL, respectively. The AFM studies show the terraces with clear atomic steps with small surface and large hexagonal pits in GaN films grown on epi-layer GaN template. We found that the density of surface defects decreases from $\sim 1.1 \times 10^9$ cm^{-2} to $\sim 4.0 \times 10^8$ cm^{-2} with the increase of the growth temperature from 730 °C to 750 °C. The PL spectra were measured for indentifying the nature of the defect states contributing to the band gap region. We observed that the concentration of the defect levels strongly depend on growth temperature. The variation of deep level defect distribution at different growth temperature and its correlation with defects density has been discussed.

II. EXPERIMENTAL DETAILS

The epitaxial GaN films were grown in RIBER PAMBE system which consist growth and preparation chambers. The base pressure in the growth chamber was better than 5×10^{-11} Torr. The growth chamber is equipped with reflection high energy electron diffraction (RHEED), standard effusion cell for Ga evaporation and a radio-frequency (RF) nitrogen plasma source to supply nitrogen radicals. The growth substrates are commercially available Lumilog n-type 3.5 μm thick epi-layer GaN templates grown by MOCVD on 2 inch c-plane sapphire. The back side of the template is coated with 1 μm thick Mo layer to increase the heat absorption from infra-red radiation heater and to obtain a uniform heat distribution. The templates were cleaned using standard organic solvents and de-ionized water. Prior to growth, the substrate was degassed for several hours at 300 °C in the preparation chamber, followed by 2 hour degassing at 700 °C in the main growth chamber. For all samples grown in this work, the nitrogen plasma with RF power of 400 Watt was used to supply nitrogen radicals during GaN growth. The nitrogen leak valve was set to produce a chamber pressure of 1.5×10^{-5} Torr. All GaN samples were grown on templates under Ga/N ratio ~ 1 condition at three different growth temperatures, 730 °C (sample 1), 740 °C (sample 2) and 750 °C (sample 3). The substrate temperature was measured by the optical pyrometer on the GaN surface. Even though the uncertainty in the temperature measurement can be as large as ±5 °C, it will be constant for all quoted growth temperatures. *In-situ* monitoring of the growth process was done by RHEED technique. The streaky RHEED pattern was obtained during GaN growth process which indicates near stoichiometric two-dimensional layer-by-layer growth of GaN film. The GaN growth rate and overall growth duration for all samples is $\sim$ 400 nm/h and 3 hrs, respectively.

The polarity of MBE grown GaN epitaxial films were determined using chemical etching in KOH solution (KOH:H_2O = 1:5 in weight ratio) for 30 min followed by the surface characterization using AFM. We did not observe any changes in surface morphologies on GaN samples after chemical etching (not shown here). It has been previously reported that the Ga-polar surface is chemically inert to KOH solutions while N-polar surface offers a continuous etching, independent of the GaN deposition techniques and growth conditions.[17] This observation indicates that our PAMBE grown GaN samples have Ga-polar surface.

The Multimode-V Veeco AFM was employed in tapping mode to characterize the surface morphology of epitaxial GaN films using silicon tips of curvature radii less than 10 nm. The root-mean-square (rms) roughness of PAMBE grown GaN surfaces was determined from AFM images of 2 μm × 2 μm areas. The optical properties of epitaxial GaN film grown at different growth temperatures were studied using PL spectroscopy. The PL measurements of all the samples were performed with excitation wavelength of 325 nm at room temperature. The beam was focused onto the sample mounted at 45° to the incident light. The emitted PL signals were passed through an emission monochromator and recorded using a photomultiplier tube. The spectral resolution of the monochromator was < 5 meV.

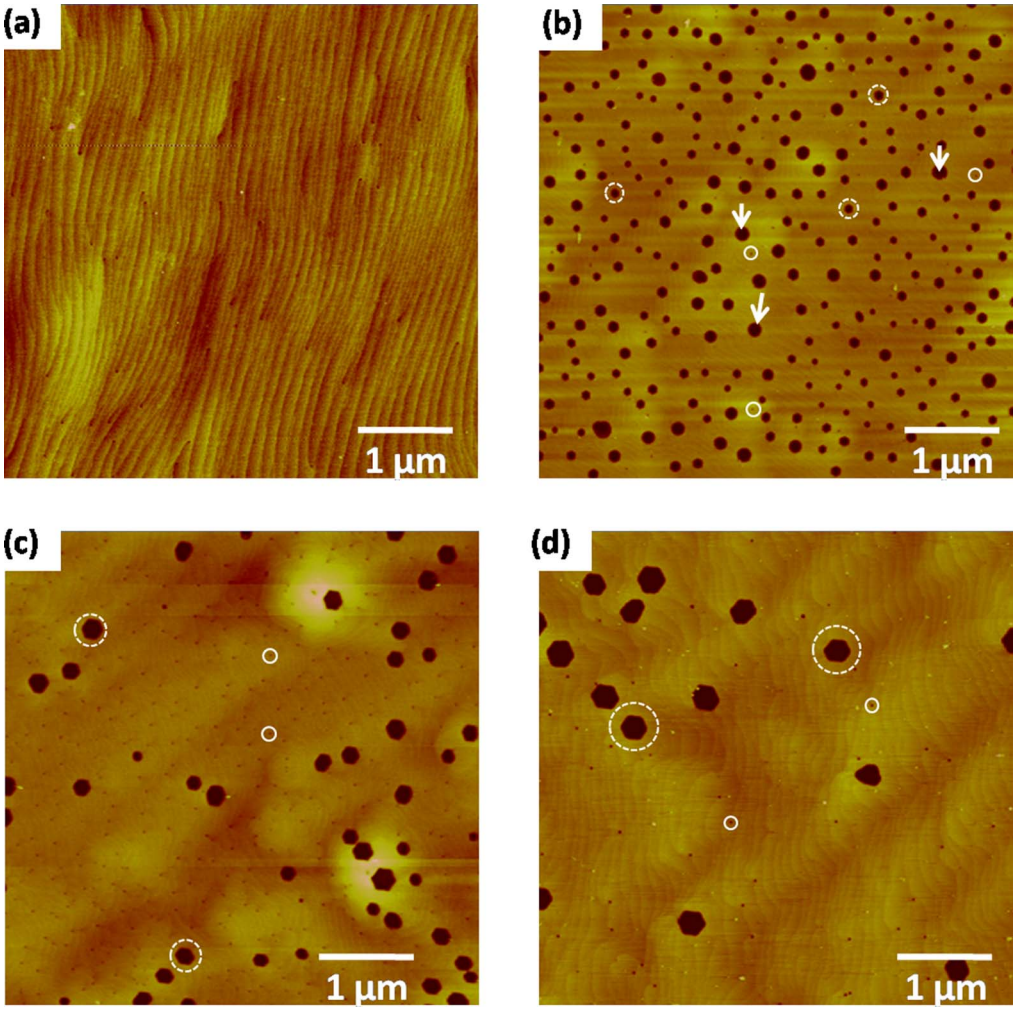

FIG. 1. (a) AFM image of the starting MOCVD grown GaN(0001) epilayer which acted as template for MBE grown GaN film. (b–d) AFM images of GaN films grown at different growth temperatures: (b) 730 °C, (c) 740 °C and (d) 750 °C. Scan area: 5 μm × 5 μm.

III. RESULTS AND DISCUSSION

A. Surface morphology of epitaxial GaN films

Surface morphologies of the epitaxial GaN film grown on epi-layer GaN on sapphire substrates at different growth temperatures were investigated using AFM in tapping mode. Figure 1(a) shows a typical AFM image of MOCVD grown 3.5 μm epi-layer GaN film on sapphire (template). The surface morphology of the GaN template was quite smooth, consisting of arrays of straight narrow (width 50–120 nm) terraces with step heights ∼ 3 Å, very similar to previous reports describing the morphology using AFM images of MOCVD grown GaN epitaxial films.[18,19] This step height agrees well with the one GaN(0001) monolayer (2.6 Å) thick layer.[20] Some of the steps are terminated tangentially at the edges of shallow depressions or pits with depth ranging 1.2–2.5 nm.

Fig. 1(b) represents the AFM image of PAMBE grown 1.2 μm thick GaN film at growth temperature 730 °C (sample 1). Our AFM image shows no spiral hillocks on the MBE grown GaN film surface which is typically obtained on the GaN surface grown by PA-MBE under Ga-rich conditions at low temperature.[19] It shows that the surface of the epitaxial grown GaN film has high surface defects and consists of terraces with step heights of one monolayer thick GaN(0001). The rms roughness value for sample 1 is 3.84 nm. Three types of defects in GaN films namely; distorted

hexagonal pits, hexagonal pits and small surface pits were observed on GaN film as shown by arrow pointer, dotted circle and solid circle in the Fig. 1(b), respectively. Step height corresponds to one monolayer thick GaN(0001) and hexagonal pit formation indicate that the epitaxial wurtzite GaN(0001) film is grown on template. The small surface pits are preferentially located at the junction between two steps. The origin of these surface pits may be due to the intersection of threading dislocations with the surface.[2,13] The hexagonal pits formation associates with the remnants of island coalescence. We would like to emphasize that different type of pits are randomly distributed over the surface of GaN films and therefore it is normal to have some areas having more pits than other areas. It was the reason that we analyzed several AFM images of same size from sample prepared in similar conditions and estimated an average number for surface defect densities from these images. The densities of distorted hexagonal pits, hexagonal pits and surface pits are $\sim 2.6 \times 10^8$ cm^{-2}, $\sim 6.2 \times 10^8$ cm^{-2} and $\sim 2.2 \times 10^8$ cm^{-2}, respectively. The total surface defects density on GaN film surface is $\sim 1.1 \times 10^9$ cm^{-2}. In addition, field emission scanning electron microscopy (FE-SEM) large scan size images (not shown here) of the all samples were also used to estimate the density of larger pits (distorted and hexagonal pits) and it matches very well with AFM measurements. The defect densities in our GaN film are comparable to the reported values.[12,15] Generally, the surface defect or dislocation densities in PAMBE grown GaN films on MOCVD grow GaN templates are in range of $\sim 10^9$–10^8 cm^{-2}.[12,15] With further increase in growth temperature and keeping all other growth parameters same, we found that the pits density progressively decreases. Fig. 1(c) represents the AFM image of 1.2 μm thick GaN film grown at 740 °C (sample 2). In this case, only two types of surface defects were obtained: hexagonal and small surface pits. The hexagonal pit density is $\sim 1.5 \times 10^8$ cm^{-2} whereas the small surface pit density is $\sim 8.3 \times 10^8$ cm^{-2}. The total pit density on sample 2 is $\sim 9.8 \times 10^8$ cm^{-2}. The rms roughness value for GaN sample 2 is 3.26 nm. The large hexagonal pits and small surface pits were observed from GaN surface grown at 750 °C (sample 3) shown in Fig. 1(d). The densities of large hexagonal pit and surface pits for sample 3 are $\sim 1.2 \times 10^8$ cm^{-2} and $\sim 2.8 \times 10^8$ cm^{-2}, respectively. The total pits density for GaN sample 3 is $\sim 4.0 \times 10^8$ cm^{-2}. The total pits density on GaN film decreases from $\sim 1.1 \times 10^9$ cm^{-2} to $\sim 4.0 \times 10^8$ cm^{-2} with increase in the growth temperature from 730 °C to 750 °C. It indicates that the surface morphology of GaN film grown using PAMBE system is sensitive to the growth temperature during growth. The density of hexagonal pits decreases with growth temperature due to the fast coalescence of islands at high growth temperature. The sample 3 has a smooth surface with rms roughness value 2.62 nm. The rms roughness values of GaN film surfaces decreases with growth temperatures. The high temperature growth condition is favorable to get less surface defects with smooth GaN film.

We have statistically analyzed the sizes and depth of the pits obtained from GaN surfaces at different growth temperatures. The lateral sizes and depth of pits were analyzed from several images on the samples prepared at the growth temperature of 730 °C as shown in Fig. 1(b) and Fig. 2(a). The distorted hexagonal pits have lateral size 110 ± 15 nm with depth of 20 ± 4 nm whereas lateral size of hexagonal pits is 80 ± 10 nm with depth of 10 ± 2 nm. The line profile across AB line in Fig. 2(a) is presented in Fig. 2(b). The line profile data also gives pictorial view of deformed hexagonal pits with more depth compared to hexagonal pits with less depth shown in Fig. 2(b). The lateral sizes of surface pits are in range of 20–35 nm with depth range of 1.2 to 3 nm. On sample 2, the hexagonal pits have lateral size 130 ± 30 nm with depth 22 ± 4 nm whereas lateral size of small surface pits is 20–35 nm with depth 1.2–4.8 nm. Depth of surface pit (Fig. 2(d)) is smaller than that of hexagonal pit as shown by line profile across line CD in Fig. 2(c). The large hexagonal pits were observed on GaN film surface grown at 750 °C (sample 3) shown in Fig. 1(d) and Fig. 2(e). The line profile across EF line in Fig. 2(e) is presented in Fig. 2(f). The large hexagonal pits have lateral size 200 ± 30 nm with depth 36 ± 5 nm whereas lateral size of small surface pits is 40–50 nm with depth 1.2–6 nm. The line profile along EF line in Fig. 2(e) is presented in Fig. 2(f) which clearly shows that the hexagonal pits on film grown at 750 °C (sample 3) have larger depths compared to that of the sample 1 and 2. The lateral sizes as well as depth of the hexagonal pits increases with increasing growth temperature. It is also observed that the terrace widths of the PAMBE grown GaN film are quite large (∼120–250 nm) for sample 3 as compared to the epi-layer GaN template, samples 1 and 2. The sizes of pits or surface defects increases whereas the growing GaN surfaces

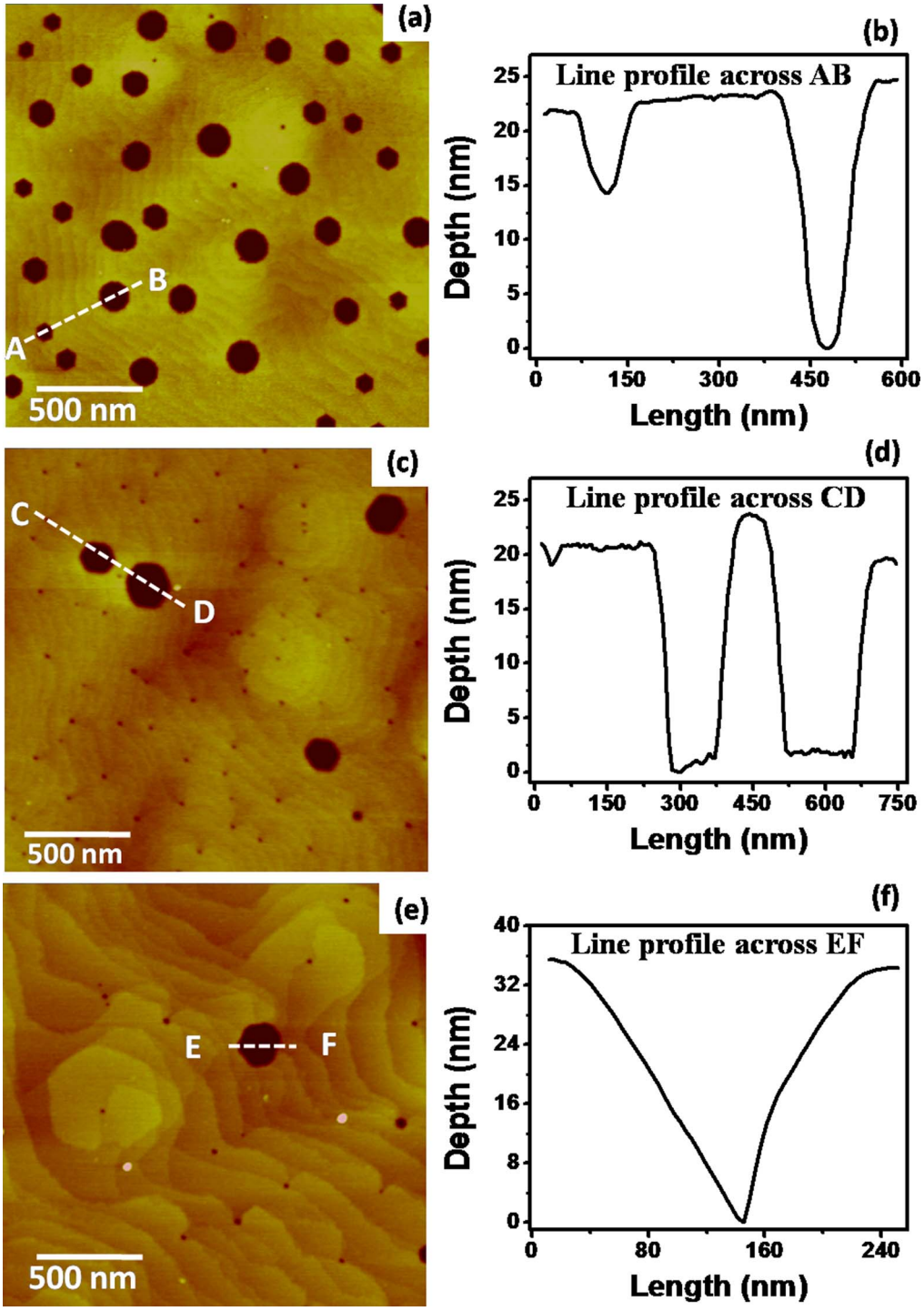

FIG. 2. (a) AFM image of GaN film grown at growth temperature 730 °C; (b) line profile across GaN film along AB line in (a). (c) AFM image of GaN film grown at growth temperature 740 °C; (d) line profile across GaN film along CD line in (c). (e) AFM image of GaN film grown at growth temperature 750 °C; (f) line profile across GaN film along EF line in (e). Scan area of all AFM images (a, c, e): 2 μm × 2 μm.

have smooth large terrace at high growth temperatures due to the interplay between the modified surface growth kinetics under the influence of thermal decomposition of GaN or desorption of Ga as well as the step-flow growth mode at high growth temperature.[21] Adelmann *et al.*[9] also reported that the Ga has been desorbed during growth of GaN at substrate temperature 740 °C with Ga/N

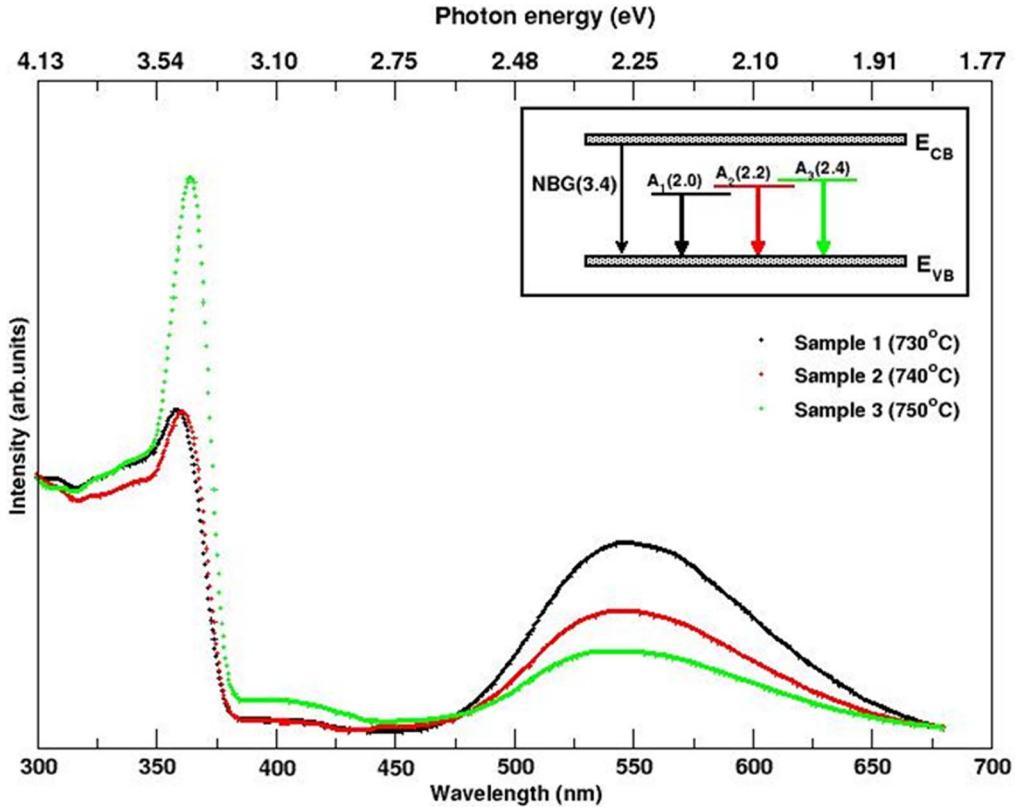

FIG. 3. PL spectra were recorded at room temperature for PAMBE grown GaN films at different growth temperatures. All the spectra have been normalized and plotted together. The inset shows a schematic diagram of the three deep center defect levels present in all the samples. The defect levels are marked by A_1, A_2 and A_3 which have been discussed in Fig. 4 and related text.

ratio $\sim$ 1. The smooth GaN surface without large pits were only obtained in step-flow growth mode at high substrate temperature in Ga rich conditions.

B. Optical properties of epitaxial GaN films

The PL spectra of epitaxial GaN films grown at three different growth temperatures are shown in Fig. 3. All the spectra were recorded at room temperature. The spectra have been collected at five different spots of the samples. Intensities of all the spectra taken from the same sample did not change substantially over most of the energy region with different spots. Since the signal intensity does not change much from spot to spot, the intensities of all the spectra taken from the same sample were averaged and plotted together. The average spectra have been normalized to the same height at nearly featureless band that extend from $\sim$ 3.93 eV (315 nm) to 4.13 eV (300 nm). The spectra consist of two dominant emission peaks, one centered at about 3.4 eV with clearly perceptible shoulders on the ultra-violet (UV) edge and another broad peak at 2.2 eV (560 nm). While the intense peak at about 3.4 eV is mainly due to the near-band-gap (NBG) related transitions, the 2.2 eV peak has been generally associated with defect related mid gap transitions (yellow luminescence, YL).[16,22–26] The UV shoulders consist of multiple weaker transitions at higher lying energy level above the conduction band minimum. We also observe a very weak feature around 2.9 eV which could be related to the blue luminescence.[23–25] The intensity of YL band is high in comparison to NBG for MOCVD grown GaN template (not shown) which indicates that the PA-MBE grown GaN samples have lower defects.

TABLE I. Summary of parameters (peak position, FWHM and normalized area) obtained by fitting the NBG peak for three GaN films grown at different growth temperatures. NBG transition spectra were fitted using a Lorentzian function. Uncertainty in determining the values of fitting parameters is estimated to be ±5%.

Sample	Near band gap transition		
	Position (eV)	FWHM (meV)	Normalized area under NBG peak
Sample 1	3.4	149	216.3
Sample 2	3.4	150	201.1
Sample 3	3.4	136	334.4

The origin of the NBG transition peak is now well known from the earlier experiments.[11,27,28] NBG region is mainly dominated by free exciton transition, donor-to-valence band transition and donor-bound exciton transitions. Thermal broadening and defect related disorder in the film also increases the broadening of the NBG peak. In order to estimate the relative changes in all the three samples due to growth temperature, we have carefully fitted the NBG region. We have used the Lorentzian line shape for fitting the NBG transition peak. Results of data fit are shown in the Table I. The full widths at half maximum (FWHM) of this transition line is 149 meV for sample 1, 150 meV for sample 2 and 136 meV for sample 3. We found that FWHM of NBG peak is lowest for sample 3 grown at 750 °C. It indicates that sample 3 is of the highest crystalline quality compared to sample 1 and 2. Improved crystallinity (lesser disorder) of sample grown at 750 °C is due to the decreased defect density as shown by AFM image analysis (Section III A).

Mid gap level broad defect related PL peak, mainly attributed with YL, centered at 2.2 eV has been reported earlier on GaN epitaxial layers grown by various methods.[7,16,22–26,29] Origin of this peak has been associated to various kinds of defect related transitions: transition from shallow donors (substitutional O and C complexes, O_N and C_N) to deep acceptors (Ga vacancies, V_{Ga}).[23–26] The intensity of this peak depends on growth conditions. The width of YL is quite large as compared to the NBG transitions peak, which is a signature of the contribution of multiple defect bands in the mid-gap region. Figure 3 clearly shows that broad peak centered at 2.2 eV decreases for samples grown at higher temperature and its intensity is minimum for sample 3 (750 °C). This observation is in good agreement with lowest defect density found for sample 3 from AFM image analysis (Section III A).

Figure 4 shows the defect-related part of the PL spectra. Defect related broad peak is usually fitted with more than one component.[30–32] In our case, minimum three peaks are required to fit the defect part of the PL spectra. We have fitted the whole defect band spectrum with three components corresponding to the three deep center defect bands contributing to this region. We have used Lorentzian line shapes for all the three fitting components, A_1 (2.0 eV), A_2 (2.2 eV) and A_3 (2.4 eV). The inset of Fig. 3 shows a schematic of the three deep center defect levels present in these samples. While fitting, we kept the energy position and FWHM of all components almost same for different samples. The position, FWHM and normalized area of each component of all the samples are listed in the Table II.

From their energy positions and range, one can assign A_1, A_2, and A_3 to mainly green, yellow and orange luminescence respectively. It is see from Table II that there is small change in relative percentage of A_1 (decreasing) and A_2 (increasing) from sample 1 to sample 3. However, contribution of YL related A_2 component is almost same for all the samples. It has been reported that intensity of YL does not depend on the density of thread dislocations and it depends on the point defect centers homogeneously distributed over GaN layer as they possess higher recombination rate than that of dislocations.[23] We have shown in section III A that even though there is a decrease in density of hexagonal pits (related to thread dislocations) from sample 1 to sample 3, large numbers of surface pits (point defects) are visible in all samples. It might be the reason that we do not see much change in the relative contribution of YL in all samples. We would like to mention that even though we have assigned A_1 and A_3 to green and orange luminescence respectively, it is not possible to comment on the basis of current data whether these have similar origin in terms of defect level transitions as

TABLE II. The fitting parameters for the defect related transition peak in PL spectra are shown. The areas of A_1, A_2 and A_3 are normalized by the total area of all the components ($A_1 + A_2 + A_3$) of the corresponding sample. The energy positions and FWHM were determined by finding the best fit common to the three peaks. The final fit for all the spectra from different samples were obtained with the same energy positions and almost same FWHM. Uncertainty in determining the values of fitting parameters is estimated to be ±5%.

	Defect band								
	A_1			A_2			A_3		
Sample	Position (eV)	FWHM (meV)	Norm. Area (%)	Position (eV)	FWHM (meV)	Norm. Area (%)	Position (eV)	FWHM (meV)	Norm. Area (%)
Sample 1	2.0	212	19.5	2.2	260	54.1	2.4	240	26.4
Sample 2	2.0	210	17.4	2.2	267	54.7	2.4	243	27.9
Sample 3	2.0	219	16.5	2.2	270	54.4	2.4	243	29.1

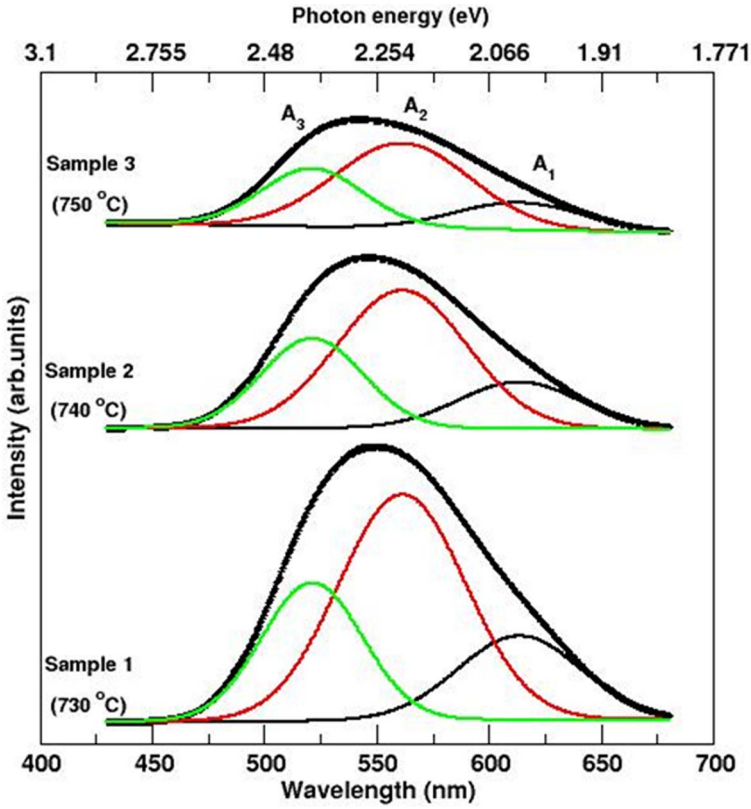

FIG. 4. Decomposition of the yellow luminescence region into three peaks is marked A_1, A_2 and A_3. The peaks A_1, A_2 and A_3 positioned at 2.0 eV, 2.2 eV and 2.4 eV, respectively. Details of the fitting are mentioned in the Table II.

of YL or there are other transitions involved. A detailed and separate study would be required to ascertain the origin of A_1 and A_3 bands.

IV. CONCLUSION

In summary, we have observed variation in the surface morphology and optical properties of the epitaxial GaN film as the growth temperature is changed. AFM images show that surface grown at growth temperature 730, 740 and 750 °C have small surface pits and large hexagonal pits. The average lateral and depth sizes of hexagonal pits increase with increasing growth temperature whereas total surface defect density decreases with growth temperature. The changes in the concentration of defects could well be connected to the growth temperature. The sample grown at 750 °C was found

with minimum defect concentration. The defect states of undoped GaN films have been probed using PL spectroscopy. FWHM and relative intensity of NBG peak of sample grown at 750 °C confirms lowest disorder in it and correlates well with our AFM results. This finding is also corroborated by the lowest intensity of defect related mid gap level peak observed for growth temperature at 750 °C. These results show that the growth temperature strongly influences the surface morphology and optical properties of the GaN epitaxial films.

ACKNOWLEDGMENTS

This work has been supported by Council of Scientific and Industrial Research (CSIR) under networking project (NWP-25). The authors are grateful to Prof. R.C. Budhani and Dr. S. T. Lakshmikumar for constant encouragement and support. Mr. Thomas Huault from RIBER, France is thanked for the technical support.

[1] K. Yamane, M. Ueno, H. Furuya, N. Okada, and K. Tadatomo, J. Cryst. Growth **358**, 1 (2012).
[2] A. Guillén-Cervantes, Z. Rivera-Álvarez, M. López-López, A. Ponce-Pedraza, C. Guarneros, and V. M. Sánchez-Reséndiz, Appl. Surf. Sci. **258**, 1267 (2011).
[3] D. Kapolnek, X. H. Wu, B. Heying, S. Keller, B. P. Keller, U. K. Mishra, S. P. DenBaars, and J. S. Speck, Appl. Phys. Lett. **67**, 154 (1995).
[4] M. Kumar, B. Roul, T. N. Bhat, M. K. Rajpalke, and S. B. Krupanidhi, Appl. Phys. Exp. **5**, 085202 (2012).
[5] R. D. Vispute, V. Talyansky, R. P. Sharma, S. Choopun, M. Downes, T. Venkatesan, K. A. Jones, A. A. Iliadis, M. A. Khan, and J. W. Yang, Appl. Phys. Lett. **71**, 102 (1997).
[6] S. S. Kushvaha, M. S. Kumar, K. K. Maurya, M. K. Dalai, and N. D. Sharma, AIP Adv. **3**, 092109 (2013).
[7] D. M. Hofmann, D. Kovalev, G. Steude, B. K. Meyer, A. Hofmann, L. Eckey, R. Heitz, T. Detchprom, H. Amano, and I. Akasaki, Phys. Rev. B **52**, 16702 (1995).
[8] G. D. Chen, M. Smith, J. Y. Lin, H. X. Jiang, M. A. Khan, and C. J. Sun, Appl. Phys. Lett. **67**, 1653 (1995).
[9] C. Adelmann, J. Brault, D. Jalabert, P. Gentile, H. Mariette, G. Mula, and B. Daudin, J. Appl. Phys. **91**, 9638 (2002).
[10] M. Leroux, N. Grandjean, B. Beaumont, G. Nataf, F. Semond, J. Massies, and P. Gibart, J. Appl. Phys. **86**, 3721 (1999).
[11] M. A. Moram, C. S. Ghedia, D. V. S. Rao, J. S. Barnard, Y. Zhang, M. J. Kappers, and C. J. Humphreys, J. Appl. Phys. **106**, 073513 (2009).
[12] H. M. Ng, D. Doppalapudi, T. D. Moustakas, N. G. Weimann, and L. F. Eastman, Appl. Phys. Lett. **73**, 821 (1998).
[13] B. Heying, I. Smorchkova, C. Poblenz, C. Elsass, P. Fini, S. DenBaars, U. Mishra, and J. S. Speck, Appl. Phys. Lett. **77**, 2885 (2000).
[14] G. Koblmuller, F. Reurings, F. Tuomisto, and J. S. Speck, Appl. Phys. Lett. **97**, 191915 (2010).
[15] J. J. M. Law, E. T. Yu, G. Koblmuller, F. Wu, and J. S. Speck, Appl. Phys. Lett. **96**, 102111 (2010).
[16] W. Grieshaber, E. F. Schubert, I. D. Goepfert, R. F. Karlicek, Jr., M. J. Schurman, and C. Tran, J. Appl. Phys. **80**, 4615 (1996).
[17] D. Li, M. Sumiya, S. Fuke, D. Yang, D. Que, Y. Suzuki, and Y. Fukuda, J. Appl. Phys. **90**, 4219 (2001).
[18] E. J. Tarsa, B. Heying, X. H. Wu, P. Fini, S. P. DenBaars, and J. S. Speck, J. Appl. Phys. **82**, 5472 (1997).
[19] B. Heying, E. J. Tarsa, C. R. Elsass, P. Fini, S. P. DenBaars, and J. S. Speck, J. Appl. Phys. **85**, 6470 (1999).
[20] V. Darakchieva, B. Monemar, and A. Usui, Appl. Phys. Lett. **91**, 031911 (2007).
[21] S. Fernández-Garrido, G. Koblmüller, E. Calleja, and J. S. Speck, J. Appl. Phys. **104**, 033541 (2008).
[22] C. Kisielowski, J. Krüger, S. Ruvimov, T. Suski, J. W. Ager III, E. Jones, Z. Liliental-Weber, M. Rubin, E. R. Weber, M. D. Bremser, and R. F. Davis, Phys. Rev. B **54**, 17745 (1996).
[23] L. Macht, J. L. Weyher, A. Grzegorczyk, and P. K. Larsen, Phys. Rev. B **71**, 073309 (2005).
[24] H. C. Yang, T. Y. Lin, and Y. F. Chen, Phys. Rev. B **62**, 12593 (2000).
[25] M. A. Reshchikov and R. Y. Korotkov, Phys. Rev. B **64**, 115205 (2001).
[26] D. O. Demchenko, I. C. Diallo, and M. A. Reshchikov, Phys. Rev. Lett. **110**, 087404 (2013).
[27] M. H. Kim, Y. C. Bang, N. Man. Park, C. J. Choi, T. Y. Seong, and S. J. Park, Appl. Phys. Lett. **78**, 2858 (2001).
[28] J. Cao, D. Pavlidis, A. Eisenbach, A. Philippe, C. B. Chevallier, and G. Guillot, Appl. Phys. Lett. **71**, 3880 (1997).
[29] S. Chichibu, T. Azuhata, T. Sota, and S. Nakamura, J. Appl. Phys. **79**, 2784 (1996).
[30] R. A. Street, Phys. Rev. B **21**, 5775 (1980).
[31] M. Omari, A. Gupta, and N. Kouklin, J. Appl. Phys. **108**, 024315 (2010).
[32] A. Hazarika, A. Layek, S. De, A. Nag, S. Debnath, P. Mahadevan, A. Chowdhury, and D. D. Sarma, Phys. Rev. Lett. **110**, 267401 (2013).